Resource Management Algorithm of Mobile Edge Computing Based on User Movement Prediction

Jin Ren (rj@ncut.edu.cn)
North China University of Technology

Jing Zhang
North China University of Technology

Research Article

Keywords: Mobile edge computing, Unscented Kalman filter, Edge servers, Mobility

Posted Date: April 19th, 2022

DOI: https://doi.org/10.21203/rs.3.rs-1537697/v1

Resource Management Algorithm of Mobile Edge Computing Based on User Movement Prediction

Jin Ren[1*] and Jing Zhang[1]

[1*]School of Information Science and Technology, North China University of Technology, Beijing, 100144, China.

*Corresponding author(s). E-mail(s): rj@ncut.edu.cn;
Contributing authors: zhjing8621@163.com;

Abstract

Abstract— In view of the uncertainty of users in the process of moving, how to effectively predict and connect stable edge servers (ESs) has become the key to solve the problem. Therefore, this paper proposes a Mobile Edge Computing (MEC) algorithm based on Unscented Kalman Filter (UKF) to predict user mobility. Firstly, the ESs with computing resources are placed on the edge or node of the network, while ensuring that the battery energy of the user is sufficient. Secondly, in the process of user motion, the motion state space, estimation model and prediction model are introduced to the distributed execution of UKF. Finally, the proposed method obtains the best prediction scheme by comparing the common prediction user mobility with the linear Kalman filter prediction user mobility. The simulation results show that the proposed method greatly improves the success rate of the task.

Keywords: Mobile edge computing, Unscented Kalman filter, Edge servers, Mobility

1 Introduction

In recent years, with the rapid development of smart phones, tablets, the Internet, the Internet of Things and other terminal equipment, the traffic carried by mobile devices is also increasing, including geographical location,

weather conditions, social data, traffic conditions [1-3]. However, due to its own processing capacity and storage capacity constraints, the user experience can not be compared with desktop operations, the emergence of mobile cloud computing technology to some extent alleviate this disadvantage. The main feature of mobile cloud computing is to build a computing storage resource pool for on-demand distribution, so that mobile devices do not need to carry out large-scale local computing and storage [4]. The location relationship between mobile terminal devices and cloud servers in mobile cloud computing network is shown in Figure 1 [5,6]. However, there are also shortcomings in mobile cloud computing, which requires data to be transmitted through the long link of mobile devices and cloud servers, which will lead to high delay caused by additional radio return load. At the same time, mobile terminals consume a lot of energy, thereby increasing the network load and bandwidth requirements [7]. In addition to the above problems faced by mobile devices, many IoT devices also face this problem when such devices transmit information due to the poor performance of processors and less storage resources [8].

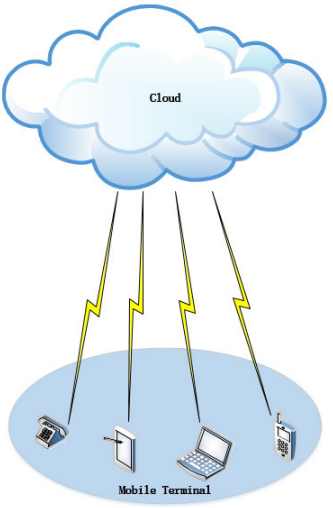

Fig. 1 Location relationship between mobile terminal devices and cloud servers in mobile cloud computing networks.

Mobile Edge Computing (MEC) provides a solution to the problem of mobile cloud computing. MEC is a new and promising computing paradigm, which has a good application in mobile terminals and the Internet of Things [9]. MEC focuses on providing services with edge cloud computing ability and information technology at the edge of mobile network, which provides a broad application prospect for 5G technology [10]. MEC is the introduction of edge devices between the mobile terminal and the cloud, and the server with mobile cloud computing function is placed on the edge of the mobile network, so as to

realize the service near the mobile terminal, which helps to reduce the frequent delay and optimize the bandwidth, and give users a better network experience [11]. The location relationship between mobile devices and cloud servers in MEC network is shown in Figure 2 [12,13].

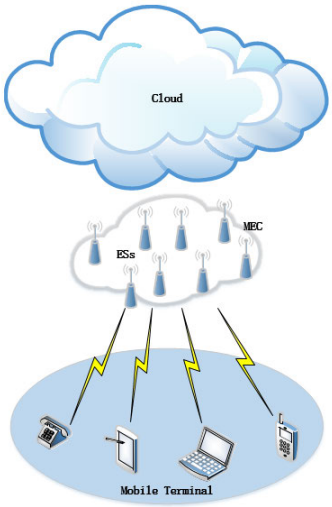

Fig. 2 Location relationship between mobile terminal devices and servers in mobile edge computing networks.

A few years ago, there was a growing concept of edge computing in the Internet called cloudlet. However, in a wide range of Internet of Things equipment distribution area can not meet the cover demand, cover wireless network still needs further construction. Nowadays, mobile edge computing plays an irreplaceable role in many aspects. In terms of mobility prediction, powerful edge computing resources provide a stable network environment for the next generation of applications, which can obtain the location information of mobile devices in real time for prediction, reduce bandwidth switching and power consumption, and allow third-party operators to provide better experience [14].

In the application scenario of mobile edge calculation, Reference [15] proposed the method of user mobility prediction, which regarded mobile users as uniform linear motion. While collecting the feedback results of task processing, it ensured the connectivity between ESs and mobile terminals, detected the matching degree between ESs prediction position and mobile user arrival point, and determined to send the task to the nearest ESs. However, in the face of the randomness of mobile users ' motion, uniform linear motion or uniform (deceleration) motion are unknown, which greatly increases the influence of noise on the accuracy of prediction position. In the face of new challenges, the above methods will not be directly applicable.

In view of the above problems, this paper proposes a mobile edge calculation algorithm based on unscented Kalman filter (UKF) to predict user mobility. In task collection, the algorithm predicts the location of mobile terminals with random motion, and requests task processing to the nearest ESs at the prediction point to ensure connectivity with mobile terminals and improve the success rate of task processing results collection. There are some improvements in latency and energy loss to ensure that the highest priority security messages are processed in the most timely manner, thereby improving user experience.

2 Motion Principle of User Mobility Prediction

2.1 Connection Model Between ESs and Mobile Terminals

ESs and mobile terminals are connected through wireless communication networks. Due to the uncertain mobility of mobile terminals, in the process of their movement, the distance between mobile terminals and ESs gradually becomes farther, so that the connection between them becomes unstable. The transmission power of ESs is limited and has a certain transmission loss, which will lead to the connection interruption between the mobile terminal and ES. As shown in Figure 3, assuming that the mobile terminal sends a request for processing tasks at location A, the mobile terminal has arrived at location B when ESs process tasks. At this time, the communication connection between the mobile terminal and ESs is interrupted due to the distance problem, so it is impossible to collect the processing results returned by ESs. The scheme adopted in this paper is to apply MEC to the scene, and the key is to use the unscented Kalman filter to predict the position of mobile terminals, so that the interruption problem of mobile terminals and ESs is effectively solved. When a mobile terminal sends a request at location A, base station observations and ESs calculations are used to predict the location of the mobile terminal receiving the processing results after the completion of the task processing, and three ESs closest to the location of the predicted receiving results (predicted location) are found to prevent their ESs from being used as an option to ensure connectivity between the mobile terminal and the ESs when an ESs cannot work properly. The accuracy of the predicted position directly determines the location of the distributed ESs, and the lower the accuracy, the worse the connectivity.

In this paper, the connectivity of ESs and mobile terminals is represented by outage probability. The outage probability can be expressed as a function of the distance between ESs and mobile terminals. We define transmission power $P_{Tx}\,[dBm]$, path loss $L\,(d)\,[dB]$, standard deviation of logarithmic normal shadow $\delta\,[dB]$, shadow gain $W\,[dB]$. The receiving power is $P_{Rx}\,[dBm]$ expressed by the following equation :

$$P_{Rx}\,(d) = P_{Tx} - L\,(d) + W \tag{1}$$

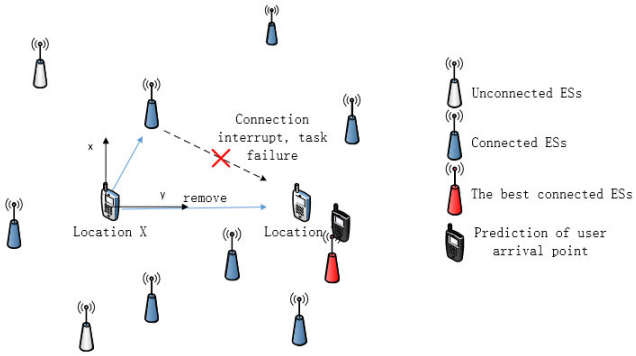

Fig. 3 Schematic diagram of connection model between ESs and mobile terminal.

$SNR\,(d)$ can be expressed as :

$$SNR\,(d) = P_{Rx}\,(d) - N_0 \tag{2}$$

Where N_0 is noise power. The probability density function of $SNR\,(d)$ obeys the normal logarithmic distribution,

$$f_{SNR(d)}\,(x) = \frac{1}{\sqrt{2\pi\alpha^2}} exp\left\{-\frac{(x-(P_{Tx}-L\,(d)-N_0))^2}{2\alpha^2}\right\}. \tag{3}$$

The outage probability, that is, the probability of receiving SNR more than $SNR\ \Gamma$, is expressed by the following equation :

$$Interrupt\ Prob\,(d) = \frac{1}{2}\left\{1 + erf\frac{\Gamma-(P_{Tx}-L\,(d)-N_0)}{\sqrt{2\alpha^2}}\right\}. \tag{4}$$

The above formula indicates that the shorter the distance between ESs and mobile terminals is, the higher the connectivity is. Then we collect task processing results at the predicted location to know the ESs closest to the predicted location. In the next section, the mobility prediction method using UKF will be introduced.

2.2 State equation of motion prediction

In reality, the mobile terminal in a period of time uniform motion and speed is not high, we can be regarded as uniform motion, but will be affected by random acceleration. We can define the position coordinates of the mobile terminal as $S_0\,(x, y)$ and the speed as $V_0\,(x, y)$, where v_x and v_y are the speeds of the mobile terminal in the X axis and Y axis respectively [16] . The state

vector of the moment is $X_t = [x, v_x, y, v_y]^T$, so the state model of the system can be obtained,

$$A = \begin{bmatrix} 1 & 0 & 0 & 0 \\ T & 1 & 0 & 0 \\ 0 & T & 1 & 0 \\ 0 & 0 & T & 1 \end{bmatrix} \quad G = \begin{bmatrix} T^2/2 & 0 \\ T & 0 \\ 0 & T^2/2 \\ 0 & T \end{bmatrix}$$

After discretization, the state equation of the system is :

$$X_t = AX_{t-1} + Gw_t \tag{5}$$

where, T is the time interval of state update, A is the state transition matrix, and the state at $t-1$ moment is transferred to the state at t moment. G is the noise driving matrix, w_t is the process noise matrix of the system, and its covariance matrix is $Q_t = E\left[w_t \ w_t^T\right]$, which is determined by the dynamic model of the system variables of each frequency component.

2.3 The observation equation of moving prediction

After discretization ,t time observation vector can be expressed as :

$$Z_t = \left[p_x \ p_y\right]^T \tag{6}$$

The dynamic observation equation in UKF dynamics can be expressed as :

$$Z_t = H\left(X_t\right) + v_t \tag{7}$$

where v_t is the measurement noise matrix of the system, and its covariance noise matrix is $R_t = E\left[v_t \ v_t^T\right]$, which is determined by the measurement noise.

3 Unscented Kalman Filter Algorithm

The unscented Kalman filtering algorithm is one of the nonlinear Kalman filtering algorithms. Unscented transformation is the core idea of the filtering algorithm, which uses Sigma sampling for linearization. Compared with Etended Kalman Filter, the estimation accuracy of UKF can reach the second-order accuracy of Taylor series expansion. Moreover, it does not use the Taylor expansion with high complexity, and adjusts the sampling frequency to reduce the error. This can handle inderivable nonlinear functions [17].

3.1 Unscented Kalman Filter Algorithm Design

The motion model of mobile terminal is a nonlinear model. The motion component of the model changes with time. It is meaningless to fit these parameters directly. A set of $2n + 1$ Sigma sampling points (n is the dimension of the system) is used to describe the Gaussian distribution of random variables, and then the posterior mean and variance of the nonlinear function are approximated by the weighted statistical linear regression technique through the transmission of the nonlinear function. The filtering value updated through the nonlinear state equation is continuously obtained.

3.1.1 Establishing System State Model

The model of system state is a nonlinear model, and the system state at t time can be obtained from the system state at $t-1$ time [18] .

$$\begin{cases} X_t = f\left(X_{t-1}, w_{t-1}\right) \\ Z_t = h\left(X_t, v_t\right) \end{cases} \tag{8}$$

Among them, X_t is the n dimensional system state matrix at t time ; Z_t is the n dimensional system observation matrix at t time; $h\left(\cdot\right)$ and $f\left(\cdot\right)$ vector functions for m and n dimensions, respectively ; w_t is the n dimensional process noise matrix, v_t is the m dimensional measurement noise matrix, and all obey the Gaussian white noise distribution with zero mean :

$$w_t \sim \left(0, Q\right) \ , \ v_t\left(0, R\right) \tag{9}$$

3.1.2 Filter State Initialization

Set X_0 as the initial state value, Q_t as the covariance of process noise, R_t as the covariance of measurement noise, the expected mean is $\overline{X_t}$, P_0 as the initial covariance matrix.

3.1.3 Gets the Sigma Test Point Set

n dimension random state vector X, with $2n+1$ Sigma test sampling point $\chi_i\left(t\right)$ $\left(i = 0, 1, 2, \cdots, n\right)$ [19,20].

$$\begin{cases} \chi_0\left(t\right) = \overline{X_t} \\ \chi_i\left(t\right) = \overline{X_t} + \left(\sqrt{\left(n+\kappa\right)P_t}\right)_i \\ \chi_{i+n}\left(t\right) = \overline{X_t} - \left(\sqrt{\left(n+\kappa\right)P_t}\right)_i \end{cases} \tag{10}$$

The corresponding mean weight W_i^m and variance weights W_i^c :

$$W_i^m = W_i^c = \begin{cases} \kappa/\left(n+\kappa\right), i = 0 \\ 1/2\left(n+\kappa\right), i \neq 0 \end{cases} \tag{11}$$

κ is the distance ratio between the mean $\overline{X_t}$ of state vector X and the sampling point set, which affects the deviation of high-order moments ; if the state dimension n continues to increase, then κ will continue to increase, resulting in nonlocal sampling effect ; it is generally necessary to meet the condition $n+\kappa = 3$; $\left(n+\kappa\right)P_t$ After *Cholesky* decomposition, the square root matrix $\left(\sqrt{\left(n+\kappa\right)P_t}\right)_.$ row or column i.

3.1.4 Calculation Time Update Equation

Through (10) and (11) obtained $2n+1$ Sigma sampling points $\chi_i'\left(t\right)$.and the corresponding mean weight $\left(W_i^m\right)'$ and variance weight $\left(W_i^c\right)'$

,$(i = 0, 1, 2, \cdots, n)$. These points are passed through the nonlinear state function $f(\cdot)$ to obtain the state estimation :

$$\chi'_{t+1/t} = f(\chi'_t) \tag{12}$$

Put $\chi'_{t+1/t}$ Substitutes (13) and (14) to obtain the estimated value of the prior state prediction $\hat{X}_{t+1/t}$ and the estimated variance $P_{t+1/t}$ of the prior state prediction, as follows :

$$\hat{X}_{t+1/t} = \sum_{i=0}^{2n} (W_i^c)' \chi'_{t+1/t} \tag{13}$$

$$P_{t+1/t} = \sum_{i=0}^{2n} (W_i^c)' \left(\chi'_{t+1/t} - \hat{X}_{t+1/t}\right) \left(\chi'_{t+1/t} - \hat{X}_{t+1/t}\right)^T + Q_t \tag{14}$$

3.1.5 Calculation of measurement update equation

Estimated value of prior state prediction based on time update equation $\hat{X}_{t+1/t}$ and estimate variance of prior state prediction $P_{t+1/t}$, input (10) and (11) get $2n + 1$ Sigma sampling points $\psi'_i(t)$, and the corresponding mean weights $(W_i^m)^*$ and variance weights $(W_i^c)^*$,$(i = 1, 2, \cdots, n)$.These points are passed through the nonlinear measurement function $h(\cdot)$ to obtain the measurement estimates:

$$\zeta'_{t+1/t} = h(\psi'_i) \tag{15}$$

Put $\zeta'_{t+1/t}$ substitute into (16) ,(17) , (18) to obtain estimates of prior measurement predictions $\hat{Z}_{t+1/t}$ and estimated variances of prior measurement predictions $P_{Z,t+1/t}$ and cross-covariances $P_{XZ,t+1/t}$, as follows :

$$\hat{Z}_{t+1/t} = \sum_{i=0}^{2n} (W_i^m)' \zeta'_{t+1/t} \tag{16}$$

$$P_{Z,t+1/t} = \sum_{i=0}^{2n} (W_i^c)' \left(\zeta'_{t+1/t} - \hat{Z}_{t+1/t}\right) \left(\zeta'_{t+1/t} - \hat{Z}_{t+1/t}\right)^T + R_{t+1} \tag{17}$$

$$P_{XZ,t+1/t} = \sum_{i=0}^{2n} (W_i^c)' \left(\chi'_{t+1/t} - \hat{X}_{t+1/t}\right) \left(\zeta'_{t+1/t} - \hat{Z}_{t+1/t}\right)^T \tag{18}$$

3.1.6 Update Kalman Filter

According $t + 1$ the estimated value of the prior measurement prediction $\hat{Z}_{t+1/t}$ and the estimated variance of the prior measurement prediction $P_{Z,t+1/t}$

and the cross-covariance substitution $P_{XZ,t+1/t}$ substitute into (19) , (20) , (21) are obtained the filtering gain K_{t+1} and the estimated value of the posterior target state $\hat{X}_{t+1/t+1}$ the estimated variance of the posterior target state $P_{t+1/t+1}$ are obtained, as follows :

$$K_{t+1} = P_{XZ,t+1/t}\left(P_{Z,t+1/t}\right)^{-1} \tag{19}$$

$$\hat{X}_{t+1/t+1} = \hat{X}_{t+1/t} + K_{t+1}\left(Z_{t+1} - \hat{Z}_{t+1/t}\right) \tag{20}$$

$$P_{t+1/t+1} = P_{t+1/t} - K_{t+1}P_{Z,t+1/t}K_{t+1}^{T} \tag{21}$$

4 Simulation Verification of Forecasting System

In order to verify the effectiveness of MEC resource management algorithm based on mobile prediction, this study uses MATLAB simulation data to verify. The simulation environment parameters are as follows : the initial position and speed of the mobile terminal are (0,100, -200,5), the requested position of the mobile terminal is (0, -180), the arrival position of the mobile terminal is (-1.224,98.4939), and the number of ESs is 5,10,20, respectively. The mobile state is randomly affected by the process noise with mean value of 0.5 and variance of 1. The mean value of the observation noise is 5, the transmission power is-10, the road stiffness loss is 4, the noise power is -95, the standard deviation of the logarithmic normal shadow is 8, the demodulation threshold is 8, the sampling period is 1 s, and the total processing time is 25 seconds. The area radius is 200 and the number of iterations is 1000. The simulation prediction results without filtering algorithm are shown in Figure 4, the simulation prediction results of linear Kalman filtering algorithm are shown in Figure 5, and the simulation prediction results of UKF filtering algorithm are shown in Figure 6.

From Figure 4 to Figure 6, the horizontal and vertical coordinates are active range, followed by X (m) and Y (m), where the blue hollow ring represents the location of ESs, the red " * " represents the location of the mobile terminal, and the pink solid triangle represents the location of the mobile terminal to send the requested signal. In Figure 4, the black solid pentagon represents the non-filtering algorithm to predict the arrival point of the mobile terminal, the black solid circle represents the position near the first arrival point predicted by the non-filtering algorithm, the blue solid circle represents the position near the second arrival point predicted by the non-filtering algorithm, and the red solid circle represents the position near the third arrival point predicted by the non-filtering algorithm. In Figure 5, the black solid pentagon represents the linear Kalman filter algorithm to predict the arrival point of the mobile terminal, the black solid circle represents the position near the first arrival point predicted by the linear Kalman filter algorithm, the blue solid circle represents the position near the second arrival point predicted by the linear Kalman filter algorithm, and the red solid circle represents the position near

the third arrival point predicted by the linear Kalman filter algorithm. In Figure 6, the black solid pentagon represents the UKF algorithm to predict the arrival point of the mobile terminal, the black solid circle represents the position near the first arrival point predicted by the UKF algorithm, the blue solid circle represents the position near the second arrival point predicted by the UKF algorithm, and the red solid circle represents the position near the third arrival point predicted by the UKF algorithm.

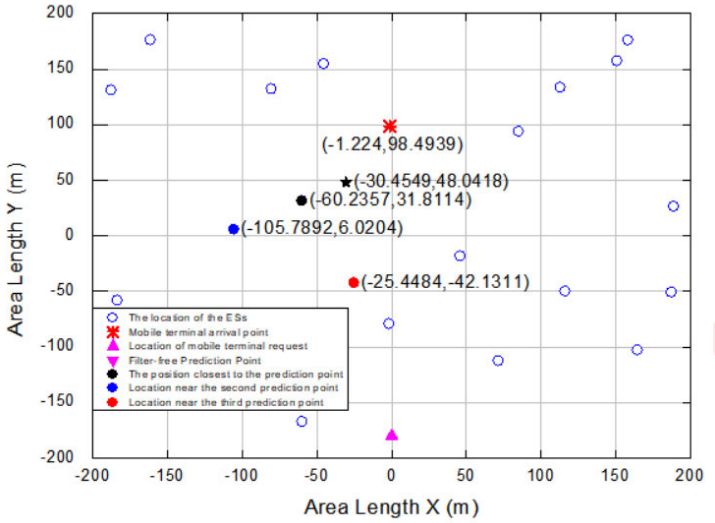

Fig. 4 Prediction point map without filtering.

The applicability of three filtering prediction methods is verified by simulation experiments. In Figure 4, the actual arrival point of non-filtering algorithm is (-1.224,98.4939), the predicted arrival point of mobile terminal is (-30.4549,48.0418), the first nearest point to the predicted arrival point of non-filtering algorithm is (-60.2357,31.8114), the second nearest point to the predicted arrival point of non-filtering algorithm is (-105.7892,6.0204), and the third nearest point to the predicted arrival point of non-filtering algorithm is (-25.4484,-42.1311). In Figure 5, the actual arrival point of the linear Kalman filter algorithm is (-1.224,98.4939), the predicted arrival point of the mobile terminal is (17.9872,60.0418), the first nearest point to the predicted arrival point of the linear Kalman filter algorithm is (84.8059,94.226), the second nearest point to the predicted arrival point of the linear Kalman filter algorithm is (45.7043,17.8282), and the third nearest point to the predicted arrival point of the linear Kalman filter algorithm is (-60.2357,31.8114).In Figure 6, the actual arrival point of UKF algorithm is (-1.224,98.4939), the predicted arrival point of mobile terminal is (5.4549,105.0418), the closest point to the predicted arrival point of UKF algorithm is (-45.6621,154.9137), the second closest point to the predicted arrival point of UKF algorithm is

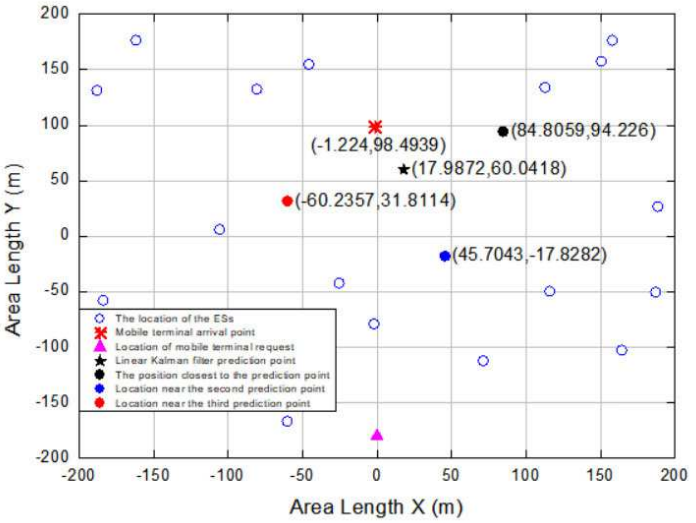

Fig. 5 Linear Kalman filter point diagram.

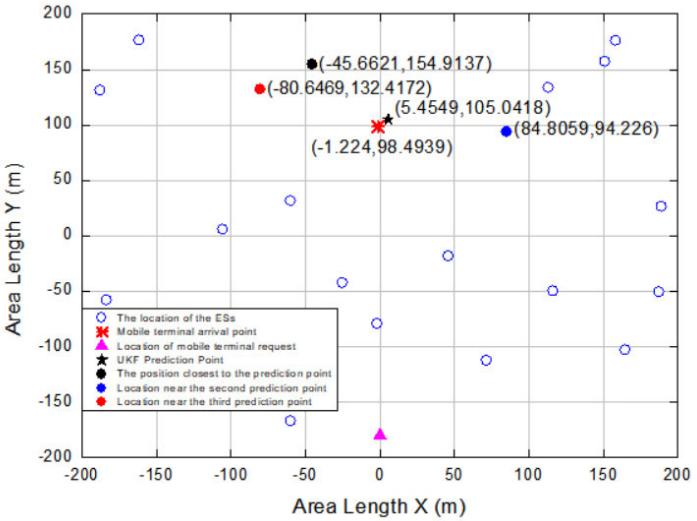

Fig. 6 UKF point diagram.

(84.8059,94.226), and the third closest point to the predicted arrival point of UKF algorithm is (-80.6469,132.4172). It can be seen from Table 1 that the coordinates of ESs points closest to the prediction point are obtained according to the three filtering methods, and then the distance and error sum between the prediction point and ESs are calculated. It can be seen that the error sum of algorithm 1, algorithm 2 and algorithm 3 is gradually reduced. Only the

Table 1 Error Sum of Three Filtering Methods

	Algorithm 1	Algorithm 2	Algorithm 3
Distance prediction point first Coordinates near ESs	(-60.2357,31.8114)	(84.8059,94.226)	(-45.6621,154.9137)
Second distance from forecast point Coordinates near ESs	(-105.7892,6.0204)	(45.7043,-17.8282)	(84.8059,94.226)
Third distance from forecast point Coordinates near ESs	(-25.4484,-42.1311)	(-60.2357,31.8114)	(-80.6469,132.4172)
Forecast point near first Distance of ESs	33.9164	75.0553	71.4154
Forecast point and second nearest Distance of ESs	86.2615	82.6558	80.0847
Forecast point near third Distance of ESs	90.3118	83.1612	90.3489
Actual arrival point and first proximity Distance of ESs	89.0446	86.1357	71.8187
The actual arrival point is close to the second one Distance of ESs	139.5895	125.4316	86.1357
Actual point of arrival and third proximity Distance of ESs	142.6962	89.0446	86.3643
Relative error sum	23.8869	15.7003	5.4571

prediction distance of algorithm 3 follows the change rule from small to large, indicating that the accuracy of the prediction position is gradually improved.

Figure 7 is the comparison chart of the error sum of the three filtering algorithms under the premise of the same number of ESs. The horizontal axis is the task of ESs processing, and the vertical axis is the error sum. The black solid line connected solid pentagon represents the sum of errors without filtering algorithm. The blue solid line connecting solid triangle represents the error sum of the linear Kalman filtering algorithm. The red solid line connecting solid circle represents the error sum of UKF algorithm. The simulation results show that when the sampling time is 1 second, the error sum of these three filtering algorithms is constantly changing, especially the error sum of UKF algorithm fluctuates in a small range. The error sum of no filtering algorithm is the highest, the error sum of linear Kalman filter algorithm is the second,

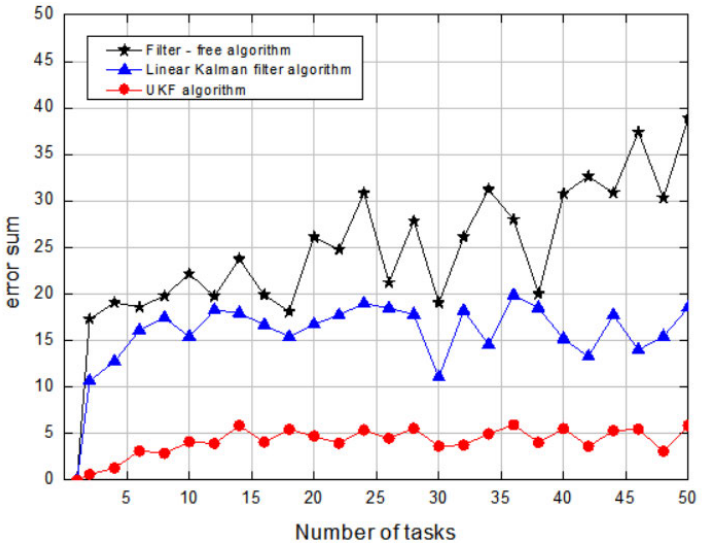

Fig. 7 Comparison of Error Sums of 3 Filtering Algorithms

and the error sum of UKF algorithm is the lowest. With the extension of sampling time, the sum of filtering error is further reduced and tends to be stable. Through continuous iteration and sampling of UKF algorithm, the optimal prediction of mobile terminal trajectory is realized.

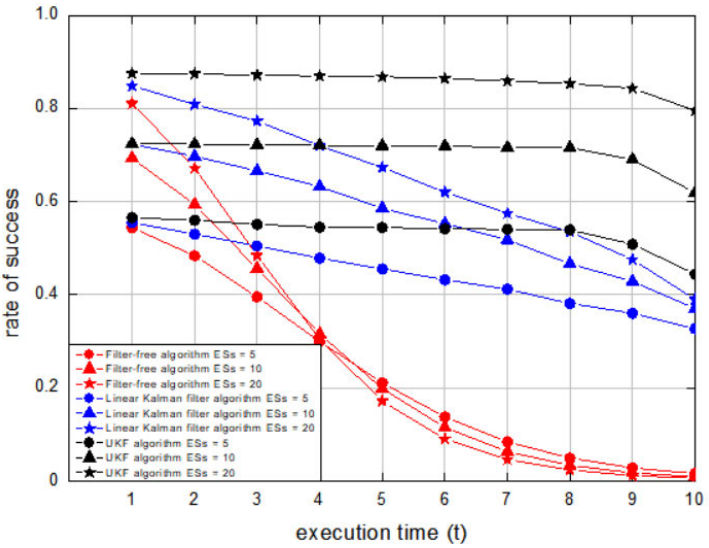

Fig. 8 Success rates of 3 algorithms

Through the above pictures and tables, the success probability of three filtering algorithms is obtained, as shown in Figure 8. The real-line connected

solid pentagon is the success rate of 20 ESs. Black represents UKF filtering algorithm, blue represents linear Kalman filtering algorithm, and red represents no filtering algorithm. The solid triangle connected by real lines is the success rate of 10 ESs. Black represents UKF filtering algorithm, blue represents linear Kalman filtering algorithm, and red represents no filtering algorithm. The solid circle connected by solid wire is the success rate under five ESs, in which black represents UKF filtering algorithm, blue represents linear Kalman filtering algorithm, and red represents no filtering algorithm. According to the nine lines above, under the same number of ESs, the success rate of no filtering algorithm is the lowest, the success rate of linear Kalman filtering algorithm is the second, and the success rate of UKF filtering algorithm is the highest. The UKF filtering algorithm is superior to the filtering effect of the linear Kalman filtering algorithm and the non-filtering algorithm. In reality, the linear Kalman filtering algorithm has the shortcomings of large sum of errors and slow filtering speed, and the UKF filtering algorithm just overcomes these shortcomings. At the same time, it reflects the advantages of strong anti-interference ability and small filtering error.

5 Conclusion

In this paper, a mobile edge computing resource management algorithm based on user mobility prediction is proposed for 5G system. Further research is done on the existing mobile terminal prediction problem. The connectivity between the mobile terminal and the ESs is reflected by the outage probability rate. The data is introduced into the UKF algorithm, and the distance between the mobile terminal and the predicted ESs is used as the observation. The system state model is established by the UKF algorithm, the filtering state initialization, the Sigma test point set is obtained, the calculation time update equation, the calculation measurement update equation and the update Kalman filter are obtained, so as to realize the best prediction of the mobile terminal trajectory. The simulation results show that the unscented Kalman filter algorithm has high accuracy in predicting the trajectory and ESs position of mobile terminals.

Declarations

Ethical Approval and Consent to participate:
Not applicable.
Human and Animal Ethics:
Not applicable.
Consent for publication:
The authors all agreed to publish this work.
Availability of supporting data:
Data sharing is not applicable to this article.
Competing interests:
There is no competing interests.

Funding:

This work was supported in part by 2022 Beijing College Students Innovation and Entrepreneurship Training Program Project, and in part by Beijing Outstanding Young Backbone Individual Project under Grant 401053712002.

Authors' contributions:

Jin Ren and Jing Zhang designed research, performed research, analyzed data, and wrote the paper.

Acknowledgements:

Thanks for the funding support.

Authors' information:

Jin Ren received the Ph.D. degree in information and communications engineering from the School of Electronic and Information Engineering, Dankook University, South Korea, in 2011. He is currently an Associate Professor with the School of Information Science and Technology, North China University of Technology. His current research interests include intelligent information processing, wireless communication, and the Internet of Things (IoT) technology.

Jing Zhang is currently pursuing her master's degree in school of Northern University of Technology, major in electronic and Communication Engineering. She holds a bachelor academic degree in Electronic Science and technology from Shenyang University of Chemical Technology. Her research interests are mainly mobile edge computing.

References

1. Lv JN , Zhang JB , Zhang ZF , Gan CQ (2020) Survey of Mobile Edge Computing Offloading Strategies. J of Chinese Comput Syst 41(9):1866-1877
2. Xue QS , Li FY (2019) A Trade-Off Task Offloading Decision Algorithm For Mobile Cloud Computing. Comput Appl and Software 36(12):66-72
3. Liu FF (2020) Research on Mobile Edge Computing Technology in 5G Network. Shanxi Electr Technology 72-75
4. Dong SQ , Li HL , Qu YB , Zhang Z , Hu L (2019) Survey of Research on Computation Unloading Strategy in Mobile Edge Computing. Comput Sci 46(11):32-40
5. Tuong VD , Truong TP , Nguyen TV , Noh W , Cho S (2021) Partial Computation Offloading in NOMA-Assisted Mobile Edge Computing Systems Using Deep Reinforcement Learning. IEEE Internet of Things J 8(17):13196-13208
6. Wang ZY , Wan YJ , Liang H (2022) The Impact of Cloud Computing-Based Big Data Platform on IE Education. Wirel Commun and Mobile Comput 1-13
7. Wu XT , Gan J , Chen SY , Zhao X , Wu YC (2021) Optimization Strategy of Task Offloading with Wireless and Computing Resource Management in Mobile Edge Computing. Wirel Commun and Mobile Comput 1-11

8. Zhou YL , He LG , Wang B , Su Y , Chen H (2020) MCAF: Developing an Annotation-Based Offloading Framework for Mobile Cloud Computing. Sci Progra 1-9
9. Huang XG , Cui YF , Zhang DY , Chen QB (2020) Joint optimization scheme of task offloading and resource allocation based on MEC. Syst Engine and Electr 42(6):1386-1394
10. Zhang XJ , Wu WG , Yang SY , Wang X (2020) Falcon:A Blockchain-Based Edge Service Migration Framework in MEC. Mobile Inform Syst 1-17
11. Zhang HB , Liu XY , Bian X , Cheng Y , Xia ST (2022) A Resource Allocation Scheme for Real-Time Energy-Aware Offloading in Vechicular Networks with MEC. Wirel Commun and Mobile Comput 1-17
12. Han QW , Huang ZY , Zeng LQ , Wu YQ , Ye L , Zu H , Lei Y (2021) An MEC Architecture-Oriented Improved RRT Algorithm for Regional Trajectory Planning. Mobile Inform Syst 1-13
13. Liu T , Fang L , Gao HH (2021) Survey of Task Offloading in Edge Computing. Comput Sci 48(1):12-15
14. Yang JK , Cao JY , Liu YN (2022) Deep Learning-Based Destination Prediction Scheme by Trajectory Prediction Framework. Security and Commun Netw 1-8
15. Ojima T , Fujii T (2018) Resource Management for Mobile Edge Computing using User Mobility Prediction. Int Conference on Inform Net,Chiang Mai,Thailand 718-720
16. Luo ZH , Chen JW , Jiang N , Liu YD (2020) Unmanned Aerial Vehicle Tracking Algorithm Based on Unscented Kalman Filter. J of Chengdu University(Natural Sci Edition) 39(1):56-59
17. Zhang YG , Huang YL , Wu ZM , Li N (2014) A High Order Unscented Kalman Filtering Method. Acta Automa Sinica 45(5):838-848
18. Lu DH , Fu HD , Wang J , Cai YX , Song SL (2021) Measurement method of ship's heave motion information based on IMU and UKF algorithm. J of Beijing University of Aeronautics and Astronautics 47(7):1323-1331
19. Chen DH , Wang C , Zhu ZK , Zou ZM (2020) Lithium battery state-of-charge estimation based on interactive multimodel unscented kalman filter Algorithm. Energy Storage Sci and Technology 9(1):257-265
20. Chen MQ , Fu JY (2021) Flight Track Prediction Method Based on Unscented Kalman Filter. Comput Simulation 38(6):27-31